

---

# PHYSARUM POWERED DIFFERENTIABLE LINEAR PROGRAMMING LAYERS AND APPLICATIONS

---

**Zihang Meng**

Dept. of Computer Sciences  
University of Wisconsin - Madison  
zihangm@cs.wisc.edu

**Sathya N. Ravi**

Dept. of Computer Science  
University of Illinois at Chicago  
sathya@uic.edu

**Vikas Singh**

Dept. of Biostatistics and Med. Informatics  
Dept. of Computer Sciences  
University of Wisconsin - Madison  
vsingh@biostat.wisc.edu

## ABSTRACT

Consider a learning algorithm, which involves an internal call to an optimization routine such as a generalized eigenvalue problem, a cone programming problem or even sorting. Integrating such a method as layers within a trainable deep network in a numerically stable way is not simple – for instance, only recently, strategies have emerged for eigendecomposition and differentiable sorting. We propose an efficient and differentiable solver for general linear programming problems which can be used in a plug and play manner within deep neural networks as a layer. Our development is inspired by a fascinating but not widely used link between dynamics of slime mold (physarum) and mathematical optimization schemes such as steepest descent. We describe our development and demonstrate the use of our solver in a video object segmentation task and meta-learning for few-shot learning. We review the relevant known results and provide a technical analysis describing its applicability for our use cases. Our solver performs comparably with a customized projected gradient descent method on the first task and outperforms the very recently proposed differentiable CVXPY solver on the second task. Experiments show that our solver converges quickly without the need for a feasible initial point. Interestingly, our scheme is easy to implement and can easily serve as layers whenever a learning procedure needs a fast approximate solution to a LP, within a larger network.

## 1 Introduction

A wide spectrum of problems in computer vision and machine learning can be expressed as, or otherwise involve as a sub-routine, the minimization of a linear function constrained by a set of linear equality and inequality constraints, also known as a Linear Program (LP). LPs can be solved efficiently even when the problem sizes are large, and industrial strength solvers are readily available. Over the last twenty years, direct applications of LPs in vision include stereo, image segmentation [16], alignment [39], optical flow [57], image reconstruction [66], denoising [61], deconvolution [2] surface reconstruction [26], graphical models [48], scene/view understanding [41], and numerous others. While the use of specialized solvers based on combinatorial optimization rather than the direct use of a simplex or interior point method has been more common in vision, there are also numerous instances where LP duality inspired schemes (such as primal-dual methods) have led to competitive and/or more general solution schemes [47].

**Why are LPs needed in the modern era?** Within the last decade, deep neural networks have come to dominate a broad gamut of problems we study in vision. So, an LP (or other well-studied “foundational” methods) will rarely provide an *end-to-end* model for a practical image understanding problem. Nonetheless, similar to how various linear algebra routines such as eigendecomposition still play a key role as a sub-routine in modern learning tasks, *LP type models are still prevalent* in numerous pipelines in vision. For instance, consider a representation learner defined by taking our favorite off-the-shelf architecture where the representations are used to setup the cost for a “matching”

problem (commonly written as a LP). Then, once a matching problem is solved, we route that output to pass through downstream layers and finally the loss is evaluated. Alternatively, consider the case where we must reason about (or group) a set of low-level primitives, via solving an assignment problem, to define a higher order semantic construct as is often the case in capsule networks [52]. Or, our architecture involves estimating the Optimal transport distance [53, 13, 54] where the cost matrix depends on the outputs of previous layers in a network. Such a module (rather, its approximations) lie at the heart of many popular methods for training generative adversarial networks (GANs) [7]. Separately, confidence calibration is becoming an increasingly important issue in deep learning [27, 45, 67]; several forms of calibration involve solutions to LPs. One approach to dealing with such a “in the loop” algorithmic procedure [4] is to treat it as a two-level optimization which leads to various efficiency issues. Of course, if the LP did not include any constraints, the optimization scheme could be unrolled. This is not as simple in the case of constraints where one must also concurrently perform projections on to the feasible set. An ideal solution would be a LP module that could be used anywhere in our architecture: one which takes its inputs from the previous layers and feeds into the subsequent layers in the network seamlessly.

**Contributions: Backpropagation through LP.** The key difficulty in solving LP within a deep network is efficiently minimizing a loss  $\ell(\cdot)$  which depends on a parameter derived from the solution of a LP – we must backpropagate through the LP solver to update the network weights. This problem is, of course, not unique to LPs but has been recently encountered in inserting various optimization modules as layers in a neural network, e.g., reverse mode differentiation through an ODE solver [17], differentiable sorting [42] and formulating quadratic [4] or cone programs as neural network layers [1]. Our inspiration is a beautiful link [59] between dynamics of a slime mold (physarum polycephalum) and mathematical optimization that has received little attention in deep learning. Exploiting the ideas in [59] with certain adjustments leads to a “LP module/layers” called  $\gamma$ -AuxPD that can be incorporated within various architectures. Specifically, our main theoretical result in Thm. 1 together with the results in [59] shows that  $\gamma$ -AuxPD can solve a much larger class of LPs. Some immediate advantages of  $\gamma$ -AuxPD include **(a)** simple plug-and-play differentiable LP layers; **(b)** converges fast; **(c)** does not need a feasible solution as an initialization **(d)** very easy to implement (less than 10 lines of code). We demonstrate how these properties provide a practical and easily usable module for solving LPs.

## 1.1 Related Works

The challenge in solving an optimization or a black-box numerical module *within* a deep network often boils down to the specific steps and the end-goal of that module itself. In some cases (unconstrained minimization of simple functions), the update steps can be analytically calculated [20, 56]. For more general unconstrained objectives, we must perform unrolled gradient descent during training [5, 44, 25]. When the optimization involves certain constraints, one must extend the frameworks to use iterative schemes incorporating projection operators, that repeatedly project the solution into a subspace of feasible solutions [72]. Since such operators are difficult to differentiate in general, it is not straight forward to incorporate them directly outside of special cases. To this end, [5] dealt with constraints by incorporating them in the Lagrangian and using the KKT conditions. In other cases, when there is no associated objective function, some authors have reported some success with using reparameterizations for homogeneous constraints [22], adapting Krylov subspace methods [51] and so on.

Our goal here is to incorporate an LP as a module within the network, and is related in principle to some other works (both in and outside of vision) that incorporate optimization routines of different forms within a deep model which we briefly review here. In [10], the authors proposed a novel structured prediction network by solving an energy minimization problem within the network whereas [43] utilized differentiable dynamic programming for structured prediction and attention. To stabilize the training of Generative Adversarial Networks (GANs), [44] defined the generator objective with respect to an unrolled optimization of the discriminator. Recently, it has been shown that incorporating concepts such as fairness [55] and verification [38] within deep networks also requires solving an optimization model internally. Closely related to our work is OptNet [4], which showed how to design a network architecture that integrates constrained Quadratic Programming (QP) as a differentiable layers but their implementation does not directly work for linear programs (quadratic term needs to be positive semidefinite). More recently, [1] introduces a package for differentiable constrained convex programming, which includes linear programs as a special case. The reader will see that compared to the above approach, our solution is arguably more direct and much simpler while maintaining efficiency.

## 2 Why Physarum Dynamics (and not something else)?

Consider a Linear Program (LP) in the standard form given by,

$$\min_{x \in \mathbb{R}^n} c^T x \quad \text{s.t.} \quad Ax = b, x \geq 0 \quad (1)$$

where  $A \in \mathbb{R}^{m \times n}$ ,  $c \in \mathbb{R}_{>0}^n$ ,  $b \in \mathbb{R}^m$ . In (1),  $c$  is called the *cost vector*, and the intersection of the linear equalities  $Ax = b$ , and inequalities  $x \geq 0$  is called the *feasible set* denoted by  $P$ . We will now briefly discuss the two main families of algorithms that are most commonly used to solve LPs of the form (1).

## 2.1 Simplex Algorithms: The Workhorse

Recall that by the Minkowski-Weyl theorem,  $P$  can be decomposed into a finite set of extreme points and rays. A family of algorithms called *Simplex* exploit this decomposition of  $P$  to solve LPs. Intuitively, a Simplex method is based on the principle that if there exists a solution to a LP, then there is at least one vertex (or an extreme point) of  $P$  that is optimal. In fact, Simplex algorithms can be seen as **First Order** methods with a careful choice of update direction so as to move along the edges of  $P$ . There are three key properties of simplex algorithms to solve LP (1): (i) *The Good*: We can obtain *exact* solutions in finite number of iterations; (ii) *The Bad*: The worst case complexity is exponential in  $m$  (or  $n$ ); and (iii) *The Ugly*: The update directions are computed by forming the *basis* matrix making the algorithm **combinatorial/nondifferentiable** in nature.

**Remark 1.** *It may not be possible to use a differentiable update rule since it would require an enumeration of vertices of  $P$  – exponential in dimensions  $n$  [9].*

## 2.2 Interior Point Algorithms: Trading Exactness for Efficiency

Asking for exact solutions of LP (1) may be a stringent requirement. An approximate solution of LP (1) can be computed using a different family of methods called *Interior Point Method* (IPM) in  $O(\sqrt{\max(m, n)})$  [69]. Intuitively, while the iterates of a simplex method goes along the edges of  $P$ , an IPM passes through the interior of this polyhedron. In particular, IPMs are **second order** algorithms since they directly solve the system of nonlinear equations derived from KKT conditions by applying variants of Newton’s method [69]. As with Simplex methods, we point out to three key properties of IPM: (i) *The Good*: IPM based algorithms can efficiently solve LP (1) in theory [37, 24]; (ii) *The Bad*: IPMs *needs* to be started from a feasible point although there are special infeasible start IPMs [50]; and (iii) *The Ugly*: In practice, IPMs are faster than Simplex Method *only* when  $m$ , and  $n$  are in millions [19].

**Remark 2.** *Even if we were able to find a feasible point efficiently, it is hard to warm start IPM methods due to the high sensitivity of the central path equation [31]. In contrast, first order methods like Simplex can be easily warm started [8].*

## 2.3 Physarum Dynamics (PD): Best of both worlds?

The term *Physarum Dynamics* (PD) refers to the movement of a slime mold called *Physarum polycephalum*, is studied in mathematical biology for its inherent computational nature and properties that closely mirror mathematical optimization. For example, in a very interesting result, [64] showed that the slime mold can solve a shortest path problem on a maze. Further, the temporal evolution of Physarum has been used to learn robust network design [62, 30], by connecting it to a broad class of dynamical systems for basic computational problems such as shortest paths and LPs. In [59], the authors studied the convergence properties of PD for LPs, and showed that these steps surprisingly mimic a steepest-descent type algorithm on a certain Riemannian manifold. While these interesting links have not been explored in deep learning, we find that the simplicity of these dynamics and its mathematical behavior provide an excellent approach towards our key goal.

We make the following mild assumption about LPs (1) that we consider here

**Assumption 1** (Feasibility). *The feasible set  $P := \{x : Ax = b, x \geq 0\}$  of (1) is nonempty.*

For the vision applications that we consider in this paper, Assumption 1 is always satisfied. We now describe the PD for solving LPs and illustrate the similarities and differences between PD and other methods.

Consider any vector  $x \in \mathbb{R}^n$  with  $x > 0$  and let  $W \in \mathbb{R}^{n \times n}$  be the diagonal matrix with entries  $\frac{x_i}{c_i}, i = 1, 2, \dots, n$ . Let  $L = AW A^T$  and  $p \in \mathbb{R}^n$  is the solution to the linear system  $Lp = b$ . Let  $q = W A^T p$ . The PD for a LP given by  $(A, b, c)$  is defined as,

$$\frac{dx_i(t)}{dt} = q_i(t) - x_i(t), \quad i = 1, 2, \dots, n. \quad (2)$$

Equivalently, using the definition of  $q$  we can write the *continuous* time PD compactly as,

$$\dot{x} = W(A^T L^{-1} b - c). \quad (3)$$

Theorem 1 and 2 in [59] guarantee that the above discretization (3) converges to an  $\epsilon$ –approximate solution efficiently as long as all the square determinants of  $A$  and the cost vector are polynomial in the dimensions  $m, n$ .

**Remark 3** (PD vs IPM). *Similar to IPM, PD requires us to compute a full linear system solve at each iteration. However, note that the matrix  $L$  associated with linear system in PD is completely different from the KKT matrix that is used in IPM. Moreover, it turns out that unlike most IPM, **PD can be started with an infeasible starting point**. Note that PD only requires the initial point to satisfy  $As = b$  which corresponds to solving ordinary least squares which can be easily done using any iterative method like Gradient Descent.*

**Remark 4** (PD vs Simplex). *Similar to Simplex, PD corresponds to a gradient, and therefore is a first order method. The crucial difference between the two methods, is that the metric used in PD is **geodesic** whereas Simplex uses the Euclidean metric. Intuitively, using the geodesic metric of  $P$  instead of the Euclidean metric can vastly improve the convergence speed since the performance of first order methods is dependent on the choice of coordinate system [70, 73].*

**When is PD efficient?** As we will see shortly in Section 5, in the two applications that we consider in this paper, the sub-determinant of  $A$  is *provably* small – constant or at most quadratic in  $m, n$ . In fact, when  $A$  is a node incidence matrix, PD computes the shortest path, and is known to converge extremely fast. In order to be able to use PD for a wider range of problems, we propose the following simple modification. However, since many of the vision primitives require auxiliary/slack variables in their LP (re)formulation, the convergence results in [59] do not apply since  $L$  in (3) is *not* invertible. In the next section, we discuss how to deal with noninvertibility of  $L$  using our proposed algorithm called  $\gamma$ -AuxPD (in Algorithm 1).

### 3 Dealing with Auxiliary Variables using $\gamma$ -AuxPD

Note that in the above description, we assume that  $c \in \mathbb{R}_{>0}^n$ . We now address the case where  $c_i = 0$  under the following assumption on the feasible set  $P$  of LP (1):

**Assumption 2** (Bounded). *The feasible set  $P \subseteq [0, M]^n$  or equivalently,  $x \in P \implies x_i \leq M \forall i \in [n]$ .*

Intuitively, if  $P$  is bounded, we may expect that the optimal solution set to be invariant under a sufficiently small perturbation of the cost vector along any direction. The following observation shows that this is indeed possible as long as  $P$  is finitely generated:

**Observation 1.** *Let  $\epsilon > 0$  be the given desired level of accuracy, and say  $c_i = 0$  for some  $i \in [n]$ . Recall that our goal is to find a point  $\hat{x} \in P$  such that  $c^T \hat{x} - c^T x^* \leq \epsilon$  where  $x^*$  is the optimal solution to the LP (1). Consider the  $\gamma$ -perturbed LP given by  $\{A, b, \hat{c}\}$ , where  $\hat{c}_i = c_i$  if  $c_i > 0$  and  $\hat{c}_i = \gamma$  if  $c_i = 0$ . Let  $x_2$  be an extreme point that achieves the second lowest cost to LP (1). Now it is easy to see that if  $\gamma < \frac{\delta}{n \cdot M}$  where  $\delta = c^T x_2 - c^T x^*$ , then  $x^*$  is an approximate solution of  $\{A, b, \hat{c}\}$ . Hence, it suffices to solve the  $\gamma$ -perturbed LP.*

With these modifications, we present our discretized  $\gamma$ -AuxPD algorithm 1 that solves a slightly perturbed version of the given LP.

**Remark 5.** *Note that  $\gamma$ -perturbation argument does not work for any  $P$  and  $c$  since LP (1) may be unbounded or have no extreme points.*

Observation 1 can be readily used for computational purposes by performing a binary search over  $\gamma$  **if** we can obtain a finite upper bound  $\gamma_u$ . Furthermore, if  $\gamma_u$  is a polynomial function of the input parameters  $m, n$  of LP, then Observation 1 implies that  $\gamma$ -AuxPD algorithm is also efficient. Fortunately, for applications that satisfy the bounded assumption 2, our Theorem 1 shows that a *tight* upper bound  $\gamma_u$  on  $\gamma_P$  can be provided in terms of  $M$  (diameter of  $P$ ).

**Implementation Details.** Under the Assumption 2, negative costs can be handled by replacing  $x_i = -y_i$  whenever  $c_i < 0$ , or in other words, by flipping the coordinate axis of coordinates with negative costs. Since we employ an iterative linear system solver to compute  $q$ , we project  $x$  on to  $\mathbb{R}_{\geq \epsilon}$  at the end of each iteration – this corresponds to a simple clamping operation.

## 4 Some testbeds for PD: Bipartite matching and SVMs

In order to illustrate the potential of the  $\gamma$ -AuxPD layer (Alg. 1), we consider two classes of LPs (from graph theory and statistical machine learning) common in vision and show that they can be solved using PD. These two classes of LPs are chosen because they link nicely to interesting problems in computer vision involving deep neural networks which we study in §5.

### 4.1 Bipartite Matching using Physarum Dynamics

---

**Algorithm 1:**  $\gamma$ -AuxPD Layer

---

```
1 Input: LP problem parameters  $A, b, c$ , initial point  $x_0$ , Max iteration number  $K$ , step size  $h$ , accuracy level  $\epsilon$ ,  
   approximate diameter  $\gamma_P$   
2 Set  $x_s \leftarrow x_0$  if  $x_0$  is provided else  $\text{rand}([n], (0, 1))$   
3 Perturb cost  $c \leftarrow c + \gamma_P \mathbf{1}_0$  where  $\mathbf{1}_0$  is the binary vector with unit entry on the indices  $i$  with  $c_i = 0$   
4 for  $i = 1$  to  $K$  do  
5   Set:  $W \leftarrow \text{diag}(x_s/c)$   
6   Compute:  $L \leftarrow AW A^T$   
7   Compute:  $p \leftarrow L^{-1}b$  using iterative solvers  
8   Set:  $q \leftarrow W A^T p$   
9   Update:  $x_s \leftarrow (1 - h)x_s + hq$   
10  Project onto  $\mathbb{R}_{\geq \epsilon}$ :  $x_s \leftarrow \max(x_s, \epsilon)$   
11 end  
12 Return:  $x_s$ 
```

---

Given two finite non-intersecting sets  $I, J$  such that  $|I| = m, |J| = n, n \ll m$ , and a cost function  $C : I \times J \rightarrow \mathbb{R}$ , solving a minimum cost bipartite matching problem corresponds to finding a map  $f : I \rightarrow J$  such that total cost  $\sum_i C(i, f(i))$  is minimized. If we represent  $f$  using an assignment matrix  $X \in \mathbb{R}^{n \times m}$ , then a LP relaxation of the matching problem can be written in standard form (1) as,

$$\min_{(X, s_m) \geq 0} \text{tr}(CX^T) + \gamma \mathbf{1}_m^T s_m \text{ s.t. } X \mathbf{1}_m = \mathbf{1}_n, X^T \mathbf{1}_n + s_m = \mathbf{1}_m \quad (4)$$

where  $C \in \mathbb{R}^{n \times m}$  is the cost matrix,  $\mathbf{1}_d$  is the all-one vector in  $d$  dimension, and  $s_m \in \mathbb{R}^m$  is the slack variable.

**Remark 6.** Note that in LP (4), the slack variables  $s_m$  impose the  $m$  inequalities given by  $X^T \mathbf{1}_n \leq \mathbf{1}_m$ .

The following theorem shows that the convergence rate of PD applied to the bipartite matching in (4) only has a dependence which is **logarithmic** in  $n$ .

**Theorem 2.** Assume we set  $0 < \gamma \leq \gamma_u$  such that  $1/\gamma_u = \Theta(\sqrt{m})$ . Then, our  $\gamma$ -AuxPD (Algorithm 1) converges to an optimal solution to (4) in  $\tilde{O}\left(\frac{m}{\epsilon^2}\right)$  iterations where  $\tilde{O}$  hides the logarithmic factors in  $m$  and  $n$ .

*Proof.* (Sketch) To prove Theorem 1, we use a result from convex analysis called the *sticky face lemma* to show that for all small perturbations of  $c$ , the optimal solution set remains invariant. We can then simply estimate  $\gamma_u$  to be the largest acceptable perturbation (which may depend on  $C, P$  but not on any combinatorial function of  $P$  like extreme points/vertices).  $\square$

**Verifying Theorem 1.** We construct random matching problems of size  $n = 5, m = 50$  (which is used in §5.1), where we randomly set elements of  $C$  to be values between  $(0, 1)$ . [1] fails to give a solution on matching problem of this size so we only compare our method with a projected gradient descent algorithm in which the projection exploits the Dykstra’s algorithm (used by [72] in section 5.1) (we denote it as PGD-Dykstra).

**Evaluation Details.** We run for 100 random instances of matching problems on both our  $\gamma$ -AuxPD algorithm and PGD-Dykstra with different number of iterations. We use the Hungarian algorithm (combinatorial search) [33] to find the optimal matching solution and compute the 2-norm between optimal solution and the solution given by our  $\gamma$ -AuxPD solver/PGD-Dykstra. Our step size is 1 and learning rate of PGD-Dykstra is set to 0.1 (both used in section 5.1.1). The results are reported in Table 1. Our  $\gamma$ -AuxPD algorithm achieves faster convergence and gets better quality solutions.

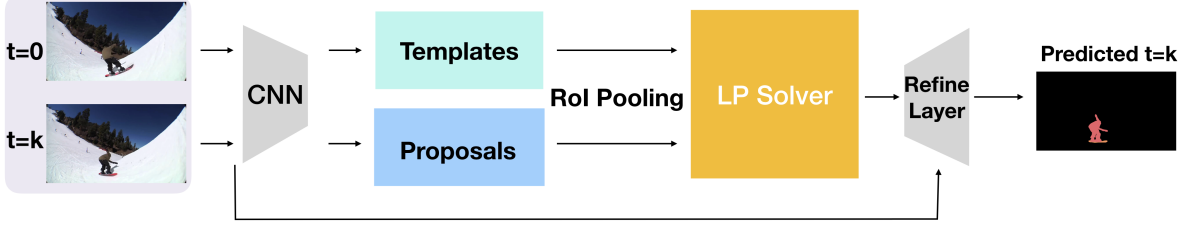


Figure 1: **Architecture of DMM [72]:** The yellow box is where the linear program is solved. In this application the linear program is a bipartite matching problem.

#### 4.2 $\ell_1$ -normalized Linear SVM using Physarum Dynamics

In the next testbed for  $\gamma$ -AuxPD, we solve a  $\ell_1$ -normalized linear SVM model [29] in the standard form of LP (1). Below,  $\tilde{K}^{[i,j]}$  stands for  $K(x_i, x_j)(\alpha_{1j} - \alpha_{2j})$ :

$$\begin{aligned}
 \min_{\alpha_1, \alpha_2, s, b_1, b_2, \xi} \quad & \sum_{i=1}^n s_i + C \sum_{i=1}^n (\xi_i + 2z_i) \\
 \text{s.t.} \quad & y_i \left( \sum_{j=1}^n y_j \tilde{K}^{[i,j]} + (b_1 - b_2) \right) + \xi_i - M z_i - l_i = 1 \\
 & \sum_{j=1}^n y_j \tilde{K}^{[i,j]} - s_i + p_i = 0, \quad \sum_{j=1}^n y_j \tilde{K}^{[i,j]} + s_i - q_i = 0, \\
 & z_i + r_i = 1, \quad \alpha_1, \alpha_2, s, b_1, b_2, \xi, z_i, l_i, p_i, q_i, r_i, \geq 0 \quad \forall i = 1, 2, \dots, n.
 \end{aligned} \tag{5}$$

Like Thm. 1, we can show a convergence result for  $\ell_1$ -SVM (5) (see supplement).

**Verifying convergence of  $\gamma$ -AuxPD for  $\ell_1$ -SVM (5).** We compare our method with the recent CVXPY solver [1] which can also solve LPs in a differentiable way. We constructed some simple examples to check whether CVXPY and our  $\gamma$ -AuxPD solver works for SVMs (e.g., binary classification where training samples of different class come from Gaussian distribution with different mean). Both  $\gamma$ -AuxPD and CVXPY give correct classification results. We will further show in section 5.2 that when used in training,  $\gamma$ -AuxPD achieves better performance and faster training time than CVXPY.

## 5 Differentiable LPs in Vision Tasks

We now demonstrate the versatility of our  $\gamma$ -AuxPD layer in particular scenarios in computer vision. Our goal here is to show that while the proposed procedure is easy, it can indeed be used in a plug and play manner in fairly different settings, where the current alternative is either to design, implement and debug a specialized sub-routine [72] or to utilize more general-purpose schemes when a simpler one would suffice (solving a QP instead of a LP) as in [36]. We try hard to keep the changes/modifications to the original pipeline where our LP solver is deployed as minimal as possible, ideally, so we should expect that there are no major fluctuations in the overall accuracy profile.

**Applications.** We evaluate the performance of  $\gamma$ -AuxPD under two different settings: **first**, as a plug-in it to facilitate a video object segmentation task [72] which needs a solution to a matching problem. **Second**, we show its use in meta learning for few shot learning [36] where the only change we need is to substitute in a model for  $\ell_1$ -SVM (which leads to a LP). We try to keep the notations mostly consistent with the original papers. Finally, while the applicability of LPs in learning and vision is vast, we nonetheless list some other applications, where alternative schemes are often adopted but  $\gamma$ -AuxPD is directly applicable.

### 5.1 Differentiable Mask-Matching in Videos

We review the key task from [72] to introduce the differentiable mask-matching network for video object segmentation, and how/why it involves a LP solution.

**Problem Formulation.** Given a video with  $T$  frames as well as the mask templates in the first frame  $R = \{r_i \mid r = 1, 2, \dots, n\}$  where  $n$  is the total number of instances throughout the video, the goal is to obtain a segmentation

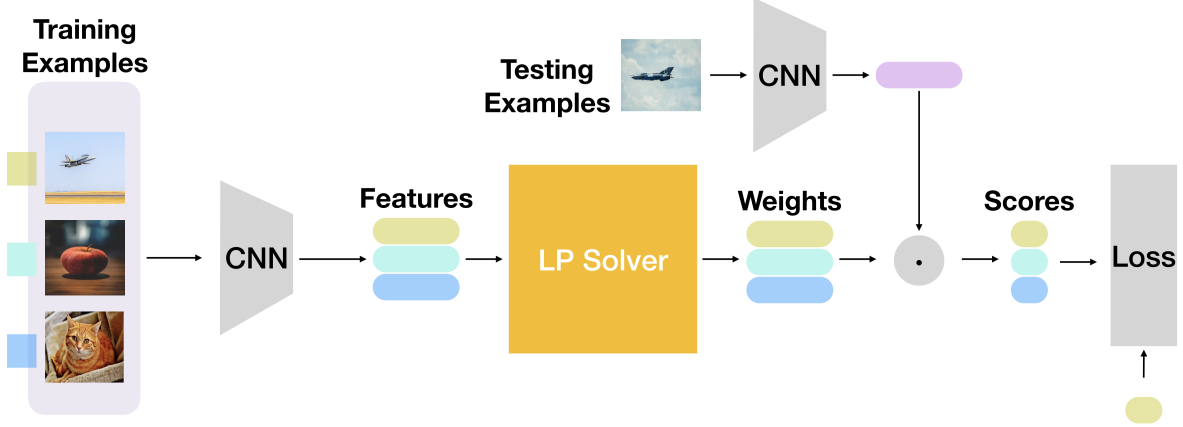


Figure 2: **Architecture of Meta-learning [36]:** The yellow box is where the linear program is solved. In this application, the linear program is a linear SVM.

for the same set of instances in all of the remaining frames in the video. Often, it is assumed that a pretrained mask proposal generation network is given (e.g., a Mask R-CNN [28]). We denote mask proposals in frame  $t$  as  $P^t = \{p_j^t \mid j = 1, \dots, m^t\}$  where  $m^t$  is the total number of proposals at time  $t$ . Note that the overall goal in [72] is to make the mask matching process differentiable so that we may obtain a learnable matching cost: the premise is that this will better handle the dramatic appearance change and deformation in the video. At time step  $t$ , a CNN denoted as  $f_\theta$  is used to extract features for the mask proposals  $P^t$  and the templates  $R$  in the first frame. For the  $i$ -th mask template  $r_i$  (ground-truth mask in the first frame) and the  $j$ -th mask proposal  $p_j^t$ , we may calculate their features as  $f_\theta(p_j^t)$ , respectively. The matching cost matrix  $C^t$  is made up of the cosine similarity between features and IoU between masks as,

$$C_{i,j}^t = (\lambda - 1) \cos(f_\theta(p_j^t), f_\theta(r_i)) - \lambda \text{IoU}(p_j^t, r_i), \quad (6)$$

where  $\lambda$  is a hyperparameter and  $0 < \lambda < 1$ . The cost matrix  $C^t$  has size  $n \times m^t$  where each row/column corresponds to a template/mask proposal respectively.

**The LP instance.** The goal is to use the cost matrix and solve a matching problem. Recall that the minimum-cost bipartite matching problem can be formulated as a integer linear programming problem (ILP) and can be relaxed to a LP, given by the formulation in standard form stated in (4) (identical to the ILP and LP in [72]). The number of proposals  $m$  is much larger than the number of templates  $n$  and so one would ask that  $X^T \mathbf{1}_n \leq \mathbf{1}_m$  instead of  $X^T \mathbf{1}_n = \mathbf{1}_m$ .

**Solver.** In [72], the authors use a specialized projected gradient descent algorithm with a cyclic constraint projection method (known as *Dijkstra's algorithm*) to solve the LP. The constraints in this LP are simple enough that calculating the projections is not complicated although the convergence rate is **not known**. We can directly replace their solver with  $\gamma$ -AuxPD in Alg. 1 to solve the problem, also in a differentiable way. Once the solution is obtained, [72] uses a mask refinement module which we also use to ensure consistency between the pipelines.

### 5.1.1 Experiments on Youtube-VOS.

We report evaluations of our  $\gamma$ -AuxPD layer on the above task.

**Dataset.** The experiments are conducted on Youtube-VOS dataset. Youtube-VOS has 3471 and 474 videos for training and validation, respectively. Among the 91 object categories in the validation set, 65 are seen in the training set while the other 26 are unseen. We follow the same experimental setting as [72].

**Training.** We used the code provided by [72] in our experiments. To evaluate our  $\gamma$ -AuxPD layer, we simply replace the PGD-Dijkstra layer with our  $\gamma$ -AuxPD layer and retrain the models from scratch. The official training dataset is divided into a train-train set and a held out train-val set which contains 200 videos. The training is performed on train-train set and evaluated on train-val set. We use the F-score and J-score as the evaluation metric.

**Parameter settings.** The projection gradient descent solver in [72] has three parameters to tune: number of gradient steps, number of projections, and learning rate. We use  $N_{grad} = 40$ ,  $N_{proj} = 5$ ,  $lr = 0.1$  as in their paper to reproduce their results. For  $\gamma$ -AuxPD layer, the choice is simple: step size  $h = 1$  and  $K = 10$  iterations work well for both two experiments and the other tests we performed. We find that [1] fails to calculate a solution on a  $5 \times 50$  matching

problem, which is needed since we use the top 50 proposals (also for reporting a sensible accuracy profile). For this reason, we do not evaluate [1]. OptNet cannot be used without non-trivial changes since it is designed to solve QPs.

#### How do different solvers compare on Youtube-VOS?

Our final results are shown in table 2. Our solver works well and since the workflow is near identical to [72], we achieve comparable results with [72] while achieving small benefits on inference time. We notice that although our solver performs better for a simulated matching problems, since the matching problem here is small and the cost matrix learned by the feature extractor is already good (so easy to solve), the runtime behavior is similar. Nonetheless, it shows that the solver can be directly plugged in and offers performance which is as good as a *specialized solution* in [72] that exploits the properties of the constraint set.

Table 2: Results on Youtube-VOS train-val split. Subscripts  $m, r, d$  stand for mean, recall, and decay respectively.

	$\mathcal{J}_m$	$\mathcal{J}_r$	$\mathcal{J}_d$	$\mathcal{F}_m$	$\mathcal{F}_r$	$\mathcal{F}_d$
DMM-Net [72]	63.4	72.7	9.3	77.3	84.9	10.5
$\gamma$ -AuxPD layer	63.4	72.2	9.2	77.3	85.3	10.4

## 5.2 Meta-learning for Few-shot Learning

We briefly review the key task from [36] to introduce the few-shot learning task using a meta-learning approach, and how it involves getting a solution to a LP.

**Problem Formulation.** Given a training set  $D^{train} = \{(x_t, y_t)\}_{t=1}^T$ , in this problem, the goal of the base learner  $\mathcal{A}$  is to estimate parameters  $\theta$  of the predictor  $y = f(x; \theta)$  so that it generalizes well to the unseen test set  $D^{test} = \{(x_t, y_t)\}_{t=1}^Q$ . It is often assumed that the training and test set are sampled from the same distribution and the domain is mapped to a feature space using an embedding model  $f_\phi$  parameterized by  $\phi$ . The parameters of the base learner can be obtained by minimizing the empirical loss with a regularizer that encourages small weights. This can be written,

$$\theta = \mathcal{A}(D^{train}; \phi) = \arg \min_{\theta} \mathcal{L}^{base}(D^{train}; \theta, \phi) + R(\theta), \quad (7)$$

where  $\mathcal{L}^{base}$  is the loss function and  $R(\theta)$  is a regularization term such as the  $\ell_1/\ell_2$  norm of the weights. The regularization term tends to be important for good generalization when training data is limited.

Meta-learning approaches for few-shot learning aim to minimize the generalization error across a distribution of tasks sampled from a task distribution. This can be thought of as performing learning from a collection of tasks instead of a single one, i.e.,  $\mathcal{T} = \{(D_i^{train}, D_i^{test})\}_{i=1}^I$ . This is referred to as a *meta-training* set [36]. Meta-learning seeks to learn an embedding model  $\phi$  that minimizes the generalization error across tasks given a base learner  $\mathcal{A}$ , written as:

$$\min_{\phi} \mathbb{E}_{\mathcal{T}} [\mathcal{L}^{meta}(D^{test}; \theta, \phi), \theta = \mathcal{A}(D^{train}; \phi)], \quad (8)$$

where we follow [36] to use the negative log-likelihood function as  $\mathcal{L}^{meta}$ . The generalization performance of the learned embedding model  $f_\phi$  is estimated on a set of *held-out* tasks (referred to as a *meta-test* set [36])  $\mathcal{S} = \{(D_j^{train}, D_j^{test})\}_{j=1}^J$ ,

$$\mathbb{E}_{\mathcal{S}} [\mathcal{L}^{meta}(D^{test}; \theta, \phi), \theta = \mathcal{A}(D^{train}; \phi)] \quad (9)$$

Due to the limited space, we refer readers to [36] for details of the meta-learning for few-shot learning task. We follow the same setting for our experiments.

**Few-shot Learning.** Standard few-shot learning evaluates models in  $K$ -way,  $N$ -shot classification tasks, where  $K$  is the number of classes and  $N$  is the number of training examples per class. Typically  $N$  is small, ranging from 1 to 5. The tuples  $(D_i^{train}, D_i^{test})$  are constructed on the fly while ensuring that  $D_i^{train} \cap D_i^{test} = \emptyset$ . In order to measure the embedding model's generalization to unseen categories, one ensures that the classes used in training, validation and test sets are mutually disjoint.

**The LP instance.** There are several requirements for the base learners. First, they need to be very fast since a base learner needs to be solved in every iteration within the *meta-learning* procedure. Second, we need to be able to estimate and backpropagate the gradient from the solution of the base learner back to the embedding model  $f_\phi$ , which means that the solver for the base learner needs to be differentiable. In [36], the authors use a multi-class linear support vector machine (SVM) with an  $\ell_2$  norm on the weights [18]. Instead, to instantiate an LP, we use a  $\ell_1$  normalized SVM proposed by [29]. The optimization model for this SVM in a standard form is shown in (5). This is a binary SVM model, on top of which we run  $\binom{k}{2}$  pairwise SVMs to obtain the solution where  $k$  is the number of classes in the task.

**Solver.** In [36], the authors use OptNet. Note that the number of parameters is only related to the number of training examples and the number of classes, which is often much smaller than the dimensionality of the features for few-shot learning. Since feature selection seems more appropriate here, we may directly replace OptNet with our  $\gamma$ -AuxPD layer to solve the  $\ell_1$ -SVM efficiently.



Table 3: Results on CIFAR-FS and FC100. Performance of more baseline methods is in supplement.

LP Solver	CIFAR-FS 5-way		FC100 5-way	
	1-shot	5-shot	1-shot	5-shot
MetaOptNet-CVXPY	$70.2 \pm 0.7$	$83.6 \pm 0.5$	$38.1 \pm 0.6$	$51.7 \pm 0.6$
MetaOptNet- $\gamma$ -AuxPD (Ours)	$71.4 \pm 0.7$	$84.3 \pm 0.5$	$38.2 \pm 0.5$	$54.2 \pm 0.5$

### 5.2.1 Experiments on CIFAR-FS and FC100

**Datasets.** The **CIFAR-FS** dataset [11] is a recently proposed few-shot image classification benchmark, consisting of all 100 classes from CIFAR-100 [32]. The classes are randomly split into 64, 16 and 20 for training, validation and testing respectively. Each class contains 600 images of size  $32 \times 32$ . The **FC100** dataset is another dataset derived from CIFAR-100 [32]. The training set contains 60 classes from 12 superclasses. The validation set contains 20 classes from 4 superclasses. The testing set contains 20 classes from 4 superclasses. Within each class, there are 600 images of size  $32 \times 32$ . We follow the code from [36] to reproduce the experiments. Training details are in supplement.

**How do different solvers compare on CIFAR-FS and FC100?** The results on CIFAR-FS and FC100 are shown in Table 1. Using the  $\ell_1$  normalized SVM, our solver achieves better performance than CVXPY [1] on both datasets and both the 1-shot and 5-shot setting. Expectedly, since the pipeline is very similar to [36], we achieve a similar performance as reported in that work, although their results were obtained through a different solver. This suggests that our simpler solver works at least as well, and no other modifications were needed. Note that during the training phase, our solver achieves  $4\times$  **improvement in runtime** compared with CVXPY (our baseline which can also solve the  $\ell_1$ -SVM). [36] also reported the performance of solving  $\ell_2$  normalized SVM. The choice of  $\ell_1$  versus  $\ell_2$  often depends on specific application settings.

We also compare the time spent on solving a batch of LP problems with  $n = 92, m = 40, p = 122$  (same size used in the experiment), where  $n$  is number of variables,  $m$  is number of equality constraints and  $p$  is the number of inequality constraints in the original problem form. Using a batch size of 8, CVXPY takes **70.5ms** seconds while our solver takes **24.2ms**; Using a batch size of 32, CVXPY takes **278.3ms** while our solver only takes **36.8ms**.

## 6 Discussion: other potential applications

Linear programming appears frequently in computer vision, and  $\gamma$ -AuxPD can be potentially applied to many settings in fairly directly. We cover a few recent examples which are interesting since they are not often attacked as a LP.

**Differentiable Calibration.** Confidence calibration is very important for many applications, such as self-driving cars [12] and medical diagnosis [35]. However, it has been well known that SVMs and deep neural networks give poor estimate of the confidence to their outputs. In general, calibration is used only as a post-procedure [27, 34]. Observe that some calibration methods can be written or relaxed in the form of a linear program. For example, Isotonic regression which is often used in vision [27, 71], fits a piecewise non-decreasing function to transform or calibrate uncalibrated outputs. By using a  $\ell_1$  loss, Isotonic regression can be written as a linear program. Therefore  $\gamma$ -AuxPD layer can be used to solve it differentially withing an end to end network during training, which may be a desirable in some cases and lead to better calibration.

**Differentiable Calculation of Wasserstein Distance (WD).** WD is widely used in many computer vision tasks, such as generative adversarial models [7] and analysis of shapes and point clouds [65]. An entropy regularized LP formulation of WD can be solved using the so-called Sinkhorn algorithm. Recent results in [3] suggest that Sinkhorn may be suboptimal since the limit of the sequence generated by the Sinkhorn algorithm may not coincide with the minimizer of the unregularized WD. Interestingly, we can apply Theorem 1 (or Theorem 1 in [59]) to conclude that PD (i) is asymptotically *exact*; and (ii) matches the convergence rate of the Sinkhorn algorithm. In the context of training deep networks, this means that we will be able to obtain unbiased gradients using  $\gamma$ -AuxPD layers which may lead to faster training.

**Differentiable Hierarchical Clustering.** Hierarchical clustering algorithms are often used in segmentation based vision tasks, see [6]. It is well known that an approximate hierarchical clustering can be computed by first rounding the optimal solution of a LP relaxation, see [14, 15]. Observe that the LP formulation of the sparsest cut problem has more constraints than decision variables owing to the ultrametric requirement of the decision variables. Hence,  $\gamma$ -AuxPD may be employed to approximately solve the Hierarchical Clustering problem, thus enabling us to differentiate through

clustering based objective functions in end-to-end deep learning frameworks. Until recently, the EM-style clustering was a bottleneck in training capsule networks [52].

**Differentiable Tracking.** [68] proposes a novel deformable surface tracking using graph matching. Recently, [20] tackles the problem of video tracking by utilizing unconstrained least squares as a subproblem which has a closed form solution. If some consistency among several sequential frames is imposed using the  $\ell_1$  norm, we directly obtain an instance that can be solved using  $\gamma$ -AuxPD.

**Differentiable Feature Matching.** Correspondences between points in images are crucial for estimating the 3D structure and camera poses in geometric computer vision tasks such as Structure-from-Motion (SfM), which is generally done by matching local features in the images. A differentiable matching layer will enable the learning of features from deep neural networks (e.g., graph neural networks) and possibly improve the matching performance. We leave this as one of our future work.

## 7 Conclusions

This paper describes how Physarum dynamics [59] based ideas can be used to obtain a differentiable LP solver that can be easily integrated within various deep neural networks where the task involves obtaining a solution to a LP. Our proposal,  $\gamma$ -AuxPD, converges quickly without requiring a feasible solution as an initialization, and is very easy to implement. Experiments demonstrate that when we preserve existing pipelines for video object segmentation and separately for meta-learning for few-shot learning, with substituting in our simple  $\gamma$ -AuxPD layer, we obtain comparable performance as more specialized schemes. The code is available for use, and complements functionality offered by tools like OptNet, NeuralODE and CVXPY. (Code will appear at <https://github.com/zihangm/Differentiable-LP-Layer>)

## 8 Acknowledgments

The authors thank Sameer Agarwal for pointing out *exact* Quasi-Newton methods [40], and for various discussions related to this work. We also thank Yingxin Jia for the useful discussions and help with experiments. This work was partially supported by NSF CAREER award (1252725) and the Center for Predictive and Computational Phenotyping (U54AI117924). Co-PI Sathya Ravi is supported by UIC-ICR start-up funds.

## References

- [1] Agrawal, A., Amos, B., Barratt, S., Boyd, S., Diamond, S., Kolter, Z.: Differentiable convex optimization layers. arXiv preprint arXiv:1910.12430 (2019)
- [2] Ahmed, A., Recht, B., Romberg, J.: Blind deconvolution using convex programming. *IEEE Transactions on Information Theory* **60**(3), 1711–1732 (2013)
- [3] Amari, S.i., Karakida, R., Oizumi, M., Cuturi, M.: Information geometry for regularized optimal transport and barycenters of patterns. *Neural computation* **31**(5), 827–848 (2019)
- [4] Amos, B., Kolter, J.Z.: Optnet: Differentiable optimization as a layer in neural networks. In: *Proceedings of the 34th International Conference on Machine Learning-Volume 70*. pp. 136–145. JMLR. org (2017)
- [5] Amos, B., Xu, L., Kolter, J.Z.: Input convex neural networks. In: *Proceedings of the 34th International Conference on Machine Learning-Volume 70*. pp. 146–155. JMLR. org (2017)
- [6] Arbelaez, P., Maire, M., Fowlkes, C., Malik, J.: Contour detection and hierarchical image segmentation. *IEEE transactions on pattern analysis and machine intelligence* **33**(5), 898–916 (2010)
- [7] Arjovsky, M., Chintala, S., Bottou, L.: Wasserstein gan. arXiv preprint arXiv:1701.07875 (2017)
- [8] Arsham, H.: Initialization of the simplex algorithm: An artificial-free approach. *SIAM Review* (1997)
- [9] Barvinok, A.: A bound for the number of vertices of a polytope with applications. *Combinatorica* (2013)
- [10] Belanger, D., McCallum, A.: Structured prediction energy networks. In: *International Conference on Machine Learning*. pp. 983–992 (2016)
- [11] Bertinetto, L., Henriques, J.F., Torr, P.H., Vedaldi, A.: Meta-learning with differentiable closed-form solvers. arXiv preprint arXiv:1805.08136 (2018)
- [12] Bojarski, M., Del Testa, D., Dworakowski, D., Firner, B., Flepp, B., Goyal, P., Jackel, L.D., Monfort, M., Muller, U., Zhang, J., et al.: End to end learning for self-driving cars. arXiv preprint arXiv:1604.07316 (2016)

- [13] Bousquet, O., Gelly, S., Tolstikhin, I., Simon-Gabriel, C.J., Schoelkopf, B.: From optimal transport to generative modeling: the vegan cookbook. arXiv preprint arXiv:1705.07642 (2017)
- [14] Calinescu, G., Karloff, H., Rabani, Y.: Approximation algorithms for the 0-extension problem. *SIAM Journal on Computing* **34**(2), 358–372 (2005)
- [15] Charikar, M., Chatziafratis, V.: Approximate hierarchical clustering via sparsest cut and spreading metrics. In: *Proceedings of the Twenty-Eighth Annual ACM-SIAM Symposium on Discrete Algorithms*. pp. 841–854. SIAM (2017)
- [16] Chen, L.C., Papandreou, G., Kokkinos, I., Murphy, K., Yuille, A.L.: Semantic image segmentation with deep convolutional nets and fully connected crfs. arXiv preprint arXiv:1412.7062 (2014)
- [17] Chen, T.Q., Rubanova, Y., Bettencourt, J., Duvenaud, D.K.: Neural ordinary differential equations. In: *Advances in neural information processing systems*. pp. 6571–6583 (2018)
- [18] Crammer, K., Singer, Y.: On the algorithmic implementation of multiclass kernel-based vector machines. *Journal of machine learning research* **2**(Dec), 265–292 (2001)
- [19] Cui, Y., Morikuni, K., Tsuchiya, T., Hayami, K.: Implementation of interior-point methods for lp based on krylov subspace iterative solvers with inner-iteration preconditioning. *Computational Optimization and Applications* (2019). <https://doi.org/10.1007/s10589-019-00103-y>, <https://doi.org/10.1007/s10589-019-00103-y>
- [20] Dave, A., Tokmakov, P., Schmid, C., Ramanan, D.: Learning to track any object. arXiv preprint arXiv:1910.11844 (2019)
- [21] Finn, C., Abbeel, P., Levine, S.: Model-agnostic meta-learning for fast adaptation of deep networks. In: *Proceedings of the 34th International Conference on Machine Learning-Volume 70*. pp. 1126–1135. JMLR. org (2017)
- [22] Frerix, T., Cremers, D., Nießner, M.: Linear inequality constraints for neural network activations. arXiv preprint arXiv:1902.01785 (2019)
- [23] Gidaris, S., Komodakis, N.: Dynamic few-shot visual learning without forgetting. In: *Proceedings of the IEEE Conference on Computer Vision and Pattern Recognition*. pp. 4367–4375 (2018)
- [24] Gondzio, J.: Interior point methods 25 years later. *European Journal of Operational Research* (2012)
- [25] Goodfellow, I., Mirza, M., Courville, A., Bengio, Y.: Multi-prediction deep boltzmann machines. In: *Advances in Neural Information Processing Systems*. pp. 548–556 (2013)
- [26] Grady, L.: Minimal surfaces extend shortest path segmentation methods to 3d. *IEEE Transactions on Pattern Analysis and Machine Intelligence* **32**(2), 321–334 (2008)
- [27] Guo, C., Pleiss, G., Sun, Y., Weinberger, K.Q.: On calibration of modern neural networks. In: *Proceedings of the 34th International Conference on Machine Learning-Volume 70*. pp. 1321–1330. JMLR. org (2017)
- [28] He, K., Gkioxari, G., Dollár, P., Girshick, R.: Mask r-cnn. In: *Proceedings of the IEEE international conference on computer vision*. pp. 2961–2969 (2017)
- [29] Hess, E.J., Brooks, J.P.: The support vector machine and mixed integer linear programming: Ramp loss svm with l1-norm regularization (2015)
- [30] Johansson, A., Zou, J.: A slime mold solver for linear programming problems. In: *Conference on Computability in Europe*. pp. 344–354. Springer (2012)
- [31] John, E., Yıldırım, E.A.: Implementation of warm-start strategies in interior-point methods for linear programming in fixed dimension. *Computational Optimization and Applications* (Nov 2008). <https://doi.org/10.1007/s10589-007-9096-y>, <https://doi.org/10.1007/s10589-007-9096-y>
- [32] Krizhevsky, A., Nair, V., Hinton, G.: Cifar-10 (canadian institute for advanced research). URL <http://www.cs.toronto.edu/kriz/cifar.html> **8** (2010)
- [33] Kuhn, H.W.: The hungarian method for the assignment problem. *Naval research logistics quarterly* **2**(1-2), 83–97 (1955)
- [34] Kuleshov, V., Fenner, N., Ermon, S.: Accurate uncertainties for deep learning using calibrated regression. arXiv preprint arXiv:1807.00263 (2018)
- [35] Ledley, R.S., Lusted, L.B.: Reasoning foundations of medical diagnosis. *Science* **130**(3366), 9–21 (1959)
- [36] Lee, K., Maji, S., Ravichandran, A., Soatto, S.: Meta-learning with differentiable convex optimization. In: *Proceedings of the IEEE Conference on Computer Vision and Pattern Recognition*. pp. 10657–10665 (2019)

- [37] Lee, Y.T., Sidford, A.: Path finding methods for linear programming: Solving linear programs in  $O(n^3)$  iterations and faster algorithms for maximum flow. In: 2014 IEEE 55th Annual Symposium on Foundations of Computer Science. IEEE (2014)
- [38] Liu, C., Arnon, T., Lazarus, C., Barrett, C., Kochenderfer, M.J.: Algorithms for verifying deep neural networks. arXiv preprint arXiv:1903.06758 (2019)
- [39] Liu, L., Yu, M., Shao, L.: Multiview alignment hashing for efficient image search. IEEE Transactions on image processing **24**(3), 956–966 (2015)
- [40] Mangasarian, O.: A newton method for linear programming. Journal of Optimization Theory and Applications **121**(1), 1–18 (2004)
- [41] Mauro, M., Riemenschneider, H., Signoroni, A., Leonardi, R., Van Gool, L.: An integer linear programming model for view selection on overlapping camera clusters. In: 2014 2nd International Conference on 3D Vision. vol. 1, pp. 464–471. IEEE (2014)
- [42] Mena, G., Belanger, D., Linderman, S., Snoek, J.: Learning latent permutations with gumbel-sinkhorn networks. arXiv preprint arXiv:1802.08665 (2018)
- [43] Mensch, A., Blondel, M.: Differentiable dynamic programming for structured prediction and attention. arXiv preprint arXiv:1802.03676 (2018)
- [44] Metz, L., Poole, B., Pfau, D., Sohl-Dickstein, J.: Unrolled generative adversarial networks (2016). arXiv preprint arXiv:1611.02163
- [45] Nixon, J., Dusenberry, M., Zhang, L., Jerfel, G., Tran, D.: Measuring calibration in deep learning. arXiv preprint arXiv:1904.01685 (2019)
- [46] Oreshkin, B., López, P.R., Lacoste, A.: Tadam: Task dependent adaptive metric for improved few-shot learning. In: Advances in Neural Information Processing Systems. pp. 721–731 (2018)
- [47] Paragios, N.K.T.: Fast primal-dual strategies for mrf optimization (2006)
- [48] Ravikumar, P., Lafferty, J.: Quadratic programming relaxations for metric labeling and markov random field map estimation. In: Proceedings of the 23rd international conference on Machine learning. pp. 737–744. ACM (2006)
- [49] Robinson, S.M.: A short proof of the sticky face lemma. Mathematical Programming **168**(1-2), 5–9 (2018)
- [50] Roos, C.: A full-newton step  $O(n)$  infeasible interior-point algorithm for linear optimization. SIAM Journal on Optimization **16**(4), 1110–1136 (2006)
- [51] de Roos, F., Hennig, P.: Krylov subspace recycling for fast iterative least-squares in machine learning. arXiv preprint arXiv:1706.00241 (2017)
- [52] Sabour, S., Frosst, N., Hinton, G.E.: Dynamic routing between capsules. In: Advances in neural information processing systems. pp. 3856–3866 (2017)
- [53] Salimans, T., Zhang, H., Radford, A., Metaxas, D.: Improving gans using optimal transport. arXiv preprint arXiv:1803.05573 (2018)
- [54] Sanjabi, M., Ba, J., Razaviyayn, M., Lee, J.D.: On the convergence and robustness of training gans with regularized optimal transport. In: Advances in Neural Information Processing Systems. pp. 7091–7101 (2018)
- [55] Sattigeri, P., Hoffman, S.C., Chenthamarakshan, V., Varshney, K.R.: Fairness gan. arXiv preprint arXiv:1805.09910 (2018)
- [56] Schmidt, U., Roth, S.: Shrinkage fields for effective image restoration. In: Proceedings of the IEEE Conference on Computer Vision and Pattern Recognition. pp. 2774–2781 (2014)
- [57] Seitz, S.M., Baker, S.: Filter flow. In: 2009 IEEE 12th International Conference on Computer Vision. pp. 143–150. IEEE (2009)
- [58] Snell, J., Swersky, K., Zemel, R.: Prototypical networks for few-shot learning. In: Advances in Neural Information Processing Systems. pp. 4077–4087 (2017)
- [59] Straszak, D., Vishnoi, N.K.: On a natural dynamics for linear programming. arXiv preprint arXiv:1511.07020 (2015)
- [60] Sung, F., Yang, Y., Zhang, L., Xiang, T., Torr, P.H., Hospedales, T.M.: Learning to compare: Relation network for few-shot learning. In: Proceedings of the IEEE Conference on Computer Vision and Pattern Recognition. pp. 1199–1208 (2018)
- [61] Tavakoli, A., Pourmohammad, A.: Image denoising based on compressed sensing. International Journal of Computer Theory and Engineering **4**(2), 266 (2012)

- [62] Tero, A., Kobayashi, R., Nakagaki, T.: A mathematical model for adaptive transport network in path finding by true slime mold. *Journal of theoretical biology* **244**(4), 553–564 (2007)
- [63] Thompson, R.C.: A determinantal inequality for positive definite matrices. *Canadian Mathematical Bulletin* **4**(1), 57–62 (1961). <https://doi.org/10.4153/CMB-1961-010-9>
- [64] Toshiyuki, N., Hiroyasu, Y., Ágota, T.: Maze-solving by an amoeboid organism. *Nature* **407**, 470 (2000)
- [65] Trillos, N.G.: Gromov-hausdorff limit of wasserstein spaces on point clouds. arXiv preprint arXiv:1702.03464 (2017)
- [66] Tsuda, K., Rätsch, G.: Image reconstruction by linear programming. In: *Advances in Neural Information Processing Systems*. pp. 57–64 (2004)
- [67] Venkatesh, B., Thiagarajan, J.J., Thopalli, K., Sattigeri, P.: Calibrate and prune: Improving reliability of lottery tickets through prediction calibration. arXiv preprint arXiv:2002.03875 (2020)
- [68] Wang, T., Ling, H., Lang, C., Feng, S., Hou, X.: Deformable surface tracking by graph matching. In: *Proceedings of the IEEE International Conference on Computer Vision*. pp. 901–910 (2019)
- [69] Wright, S.J.: *Primal-dual interior-point methods*, vol. 54. Siam (1997)
- [70] Yang, H.H., Amari, S.i.: The efficiency and the robustness of natural gradient descent learning rule. In: *Advances in neural information processing systems* (1998)
- [71] Zadrozny, B., Elkan, C.: Transforming classifier scores into accurate multiclass probability estimates. In: *Proceedings of the eighth ACM SIGKDD international conference on Knowledge discovery and data mining*. pp. 694–699 (2002)
- [72] Zeng, X., Liao, R., Gu, L., Xiong, Y., Fidler, S., Urtasun, R.: Dmm-net: Differentiable mask-matching network for video object segmentation. In: *Proceedings of the IEEE International Conference on Computer Vision*. pp. 3929–3938 (2019)
- [73] Zhang, H., Sra, S.: First-order methods for geodesically convex optimization. In: *Conference on Learning Theory* (2016)

# Physarum Powered Differentiable Linear Programming Layers and Applications: Supplement

## 1 Proof of Theorem 2 in the Main Paper

**Theorem.** Assume we set  $0 < \gamma \leq \gamma_u$  such that  $1/\gamma_u = \Theta(\sqrt{m})$ . Then, our  $\gamma$ -AuxPD converges to an optimal solution to matching problem (e.g. (4) in main paper) in  $\tilde{O}\left(\frac{m}{\epsilon^2}\right)$  iterations where  $\tilde{O}$  hides the logarithmic factors in  $m$  and  $n$ .

*Proof.* It is sufficient to show that  $\gamma_u = \Theta(\sqrt{m+n})$ . But showing such a constant exists is equivalent to showing that there is a neighborhood  $\mathcal{N} = \mathcal{B}(c, r)$  around the cost vector or objective function  $c$  of radius  $r > 0$  such that the optimal values of any two cost  $c_1, c_2 \in \mathcal{N}$  coincide i.e., there exists  $x^* \in P$  such that  $c_1^T x^* = c_2^T x^*$ . To see that this is sufficient for our purposes, note that we can add small but positive constant to all the coordinates in  $c$  that correspond to auxiliary/slack variables. Now, it is easy to see that Assumptions 1 and 2 guarantee that the optimal solution set is a *bounded* polyhedral multifunction. Hence, we can use the Sticky Face lemma [49] to guarantee that such a nonzero  $r$  exists. To conclude, we observe from the proof of the Sticky Face lemma, that  $r$  can be upper bounded by  $1/M$ , where  $M$  corresponds to the the diameter of  $P$  which is  $\Theta(\sqrt{m})$ .  $\square$

## 2 Proof of convergence of $\ell_1$ -SVM

Since the SVM formulation is always feasible, by the separating hyperplane theorem, there exists a  $\kappa > 0$  such that the when we add cost of  $\kappa$  to each coordinate of  $\alpha_1, \alpha_2, b_1, b_2, p, q, r$ , then the (cost) perturbed linear program and the original LP ((6) in the main paper), have the same optimal solution. Then, it is easy to see that  $C_s$  of this perturbed problem is quadratic in  $n, C$  and  $\kappa$ . By scaling the data points, we can assume that

$$\|x_i\|_2 \leq 1. \quad (1)$$

We now bound the magnitude of sub-determinant  $D$  of the perturbed SVM LP. First note that the slack variables are diagonal, hence, the contribution to the determinant will be at most 1. Hence, to bound  $D$ , we need to bound the determinant of the kernel matrix  $K(X, X)$ . Using Fischer’s inequality [63], we have that,

$$D \leq (K(x_i, x_i))^n. \quad (2)$$

For a linear kernel, we have that,  $D = \|x_i\|^n \leq 1$  (by assumption (1)). For a Gaussian kernel scale  $\sigma$ , we have that,  $D = O(\sigma)$  with high probability. We can easily extend this to any bounded kernel  $K$ .

## 3 More baseline results on meta-learning for few shot learning task (in addition to Table. 3 in main paper)

More baseline results (in addition to Table 3 in main paper) are shown in Table 1. We achieve comparable performance using  $\ell_1$ -SVM with [36] which uses  $\ell_2$ -SVM and surpasses previous baseline methods. The choice between  $\ell_1$  and  $\ell_2$  often depends on the specific application considered.

Table 1: More baseline results on CIFAR-FS and FC100.

LP Solver	CIFAR-FS 5-way		FC100 5-way	
	1-shot	5-shot	1-shot	5-shot
MAML [21]	58.9 $\pm$ 1.9	71.5 $\pm$ 1.0	—	—
Prototypical Networks [58]	55.5 $\pm$ 0.7	72.0 $\pm$ 0.6	35.3 $\pm$ 0.6	48.6 $\pm$ 0.6
Relation Networks [60]	55.0 $\pm$ 1.0	69.3 $\pm$ 0.8	—	—
R2D2 [11]	65.3 $\pm$ 0.2	79.4 $\pm$ 0.1	—	—
TADAM [46]	—	—	40.1 $\pm$ 0.4	56.1 $\pm$ 0.4
ProtoNets(with backbone in [36]) [58]	72.2 $\pm$ 0.7	83.5 $\pm$ 0.5	37.5 $\pm$ 0.6	52.5 $\pm$ 0.6
MetaOptNet-RR [36]	72.6 $\pm$ 0.7	84.3 $\pm$ 0.5	40.5 $\pm$ 0.6	55.3 $\pm$ 0.6
MetaOptNet-SVM [36]	72.0 $\pm$ 0.7	84.2 $\pm$ 0.5	41.1 $\pm$ 0.6	55.5 $\pm$ 0.6
MetaOptNet-CVXPY	70.2 $\pm$ 0.7	83.6 $\pm$ 0.5	38.1 $\pm$ 0.6	51.7 $\pm$ 0.6
MetaOptNet- $\gamma$ -AuxPD (Ours)	71.4 $\pm$ 0.7	84.3 $\pm$ 0.5	38.2 $\pm$ 0.5	54.2 $\pm$ 0.5

## 4 Training details on on CIFAR-FS and FC100 Dataset

For the **meta-learning setup**, we follow [36] and use a ResNet-12 network in the experiments. For the optimizer, we use SGD with Nesterov momentum of 0.9 and a weight decay of 0.0005. The mini-batch size is set to 8. The model was trained for 60 epochs, with each epoch consisting of 1000 sample tasks. The learning rate was initially set to 0.1, and then changed to 0.006, 0.0012 and 0.00024 at epochs 20, 40 and 50, respectively. During training, horizontal flip, random crop and color (brightness, contrast and saturation) jitter data augmentation were used, closely following [36, 23]. For the **Base-learner setup**, for our  $\ell_1$  normalized SVM, we use  $C = 1.0, M = 0.001$ . We used pairwise SVMs for multi class classification. For 5-way classification we have in total 10 pairwise SVMs. For our Physarum LP solver, we use 10 iterations with step size 1.0, the same setting as our previous experiment. For **Few-shot setup**, 5-way few-shot learning experiments were conducted. During training, we followed [36] and used 5-shot for CIFAR-FS and 15-shot for FC100. We report results using 1-shot and 5-shot respectively in testing.